International Journal of Impact Engineering 136 (2020) 103434

Contents lists available at ScienceDirect

International Journal of Impact Engineering

journal homepage: www.elsevier.com/locate/ijimpeng

Influence of key design parameters of ultra-high performance fibre reinforced concrete on in-service bullet resistance

P.P. Li[a], H.J.H. Brouwers[a], Qingliang Yu[a,b,*]

[a] Department of the Built Environment, Eindhoven University of Technology, P.O. Box 513, 5600MB, Eindhoven, the Netherlands
[b] School of Civil Engineering, Wuhan University, 430072, Wuhan, PR China

ARTICLE INFO

Keywords:
Ultra-high performance concrete
Bullet impact resistance
Strength class
Steel fibre
Coarse aggregate
Perforation limit

ABSTRACT

This study investigates the influence of key parameters on in-service bullet impact resistance of ultra-high performance fibre reinforced concrete (UHPFRC), with the aim to provide design guidance for the engineering applications. The effects of steel fibre type and dosage, matrix strength, coarse basalt aggregates, and target thickness are researched by subjecting the UHPFRC to a 7.62 mm bullet shooting with velocities of 843–926 m/s. The results show that the UHPFRC, designed by using a particle packing model with compressive strength around 150 MPa, is appropriate to develop protective elements considering both anti-penetration performance and cost-efficiency. The 13 mm short straight steel fibres show better anti-penetration than the 30 mm hook-ended ones, and the optimum volume dosage is approximately 2% by considering both the penetration and crack inhibition. Introducing coarse basalt aggregates with the particle size up to 25 mm into UHPFRC reduces the powder consumption from 900 kg/m^3 to 700 kg/m^3, and results in slightly higher mechanical strength and significantly enhanced bullet impact resistance with 14.5% reduction of penetration depth. The safe thicknesses (perforation limit) of the designed UHPFRC slabs are approximately 85 mm and 95 mm to withstand the 7.62 × 51 mm NATO armor-piercing bullet impact under velocity 843 mm/s and 926 mm/s, respectively.

1. Introduction

Extreme conditions or accidental loadings surrounding our human life have attracted more and more public attention, such as explosive or ballistic impact in terrorist attack, natural earthquake or hurricane disaster, vehicle impact in traffic accident, and ship collision on offshore structure or bridge [1,2]. Concrete is one of the mostly widely utilized construction materials in both civil and defence engineering, and its projectile impact properties (e.g. penetration depth, perforation, crack propagation) are always an important concern. Among the diverse types of concretes, ultra-high performance fibre reinforced concrete (UHPFRC) has great potential for protective and military applications, owing to its superior workability, mechanical strength, toughness and energy absorption capacity [3–8]. The UHPFRC has been developed since the 1990s, and its mix design and basic static properties have been extensively investigated [9–13]. However, the phase composition, microstructure and response behave very differently under impact loadings compared to static load [14–17]. Furthermore, the dynamic properties and damage patterns exhibit large differences when subjected to different impact loadings, such as drop-weight or pendulum impact, seismic effect, projectile impact, blast [1,18]. Hence, the material or even structural design principles should differ based on the different specific loading type, instead of simply considering static performance. This study aims to optimize the mix design of UHPFRC and research the influence of key parameters on ballistic impact properties subjected to the in-service 7.62 × 51 mm NATO armor-piercing bullets.

The matrix strength class greatly influences the anti-penetration performance of concrete under the high-velocity projectile impact. Many experimental results and analytical models indicated that the depth of penetration (DOP) under projectile impact has an inverse relationship with the compressive strength [19,20], which means that concrete with a higher compressive strength contributes to a better bullet impact resistance. Currently, the compressive strength of UHPFRC is usually achieved within a large range from about 120 MPa–200 MPa [3,11]. The high strength of UHPFRC can be obtained by using some special design principles, such as low water amount with high dosage of superplasticizer, large amount of cement, steel fibre addition, thermal and chemical activation, and extra pressurization treatment before final setting [9,21]. All those methods tend to enlarge the cost of UHPFRC. Thus, a better ballistic impact resistance normally goes with a sacrifice of economic benefits. How to keep a

* Corresponding author.
E-mail address: q.yu@bwk.tue.nl (Q. Yu).

https://doi.org/10.1016/j.ijimpeng.2019.103434
Received 27 September 2019; Received in revised form 29 October 2019; Accepted 30 October 2019
Available online 31 October 2019

balance between impact performance and strength/cost of UHPFRC is of great significance for its wider engineering application. This study attempts to research the effect of matrix strength on the projectile impact resistance, and then suggest an appropriate efficient matrix strength of UHPFRC in protective elements and structures.

Steel fibres are another key ingredient in UHPFRC to strengthen the bullet impact resistance. They are considerably efficient to enhance the stress transfer capability beyond elastic state and improve the energy absorption capacity [1,22]. The 'bridge effect' by the steel fibres contributes to restraining crack propagation, which decreases the damage degree and thus increases the multiple bullet striking bearing capacity. Furthermore, steel fibres significantly reduce the fragments induced by the scabbing and spalling damages, which consequently decrease the secondary harm by the concrete fragments. Meanwhile, the enhanced crack inhibition capacity by steel fibres helps to maintain the integrity of concrete target, which provides certain confinement on the impact position by outer material, and ease the inner local impact damage. However, the steel fibre reinforcement is greatly dependent on the fibre content and shape [23,24]. Moreover, the utilized high-strength steel fibres in UHPFRC are much more expensive compared to other raw materials. Therefore, steel fibres should be optimized in UHPFRC in terms of type and content by comprehensively considering the DOP, crack resistance and steel utilization efficiency, to achieve a cost-efficient protective component and structure.

Conventional UHPFRC is usually developed without applying coarse aggregates to achieve a better homogeneity and avoid the inherent stress concentration [9,10]. Recently, coarse aggregates were introduced into UHPC system, in order to reduce the cost and powder consumption, increase volume stability and even mechanical strength [5,25–28]. Furthermore, some researchers found that concrete containing coarse aggregates contributes to enhanced high-velocity projectile impact resistance, attributing to the mass abrasion and trajectory deviation of the projectile by coarse aggregates with high hardness index [19]. Zhang et al. [20] reported that coarse granite aggregates addition could reduce the DOP and crater diameter of high strength concrete by a 12.6 mm ogive-nosed projectile. Wu et al. [29,30] investigated the effects of coarse basalt and corundum aggregates on the impact resistance of UHPFRC by reduce-scaled (25.3 mm) ogive-nosed projectiles, and suggested aggregate sizes should be 1.5 times larger than the diameter of projectile. However, the ballistic impact resistance of UHPFRC with coarse aggregates by smaller projectile (e.g. the in-service 7.62 mm NATO armor-piercing bullet) should be more sensitive to the aggregates' sizes and contents, due to the high variability to hitting the mortar matrix or coarse aggregates. Thus, the effect of coarse aggregates on small bullet impact resistance should be researched and identified.

The objective of this study is to explore the influence of key parameters on impact resistance of UHPFRC subjected to the in-service 7.62 × 51 mm NATO armor-piercing bullet with velocities of 843–926 m/s, and propose a design guideline for relevant engineering applications. Five UHPFRC matrixes are designed by using a particle packing model, and 37 cylindrical targets are prepared to study the effects of steel fibre type and dosage, matrix strength, coarse basalt aggregate, and target thickness. The mechanical strength, penetration depth and damage pattern are measured and analysed. The appropriate strength class, steel fibre type and content, coarse aggregate addition are attained by comprehensively considering penetration depth, crack inhibition and cost-efficiency. Furthermore, the safety thicknesses (perforation limit) of the designed UHPFRC slabs are suggested in order to withstand the in-service 7.62 × 51 mm NATO armor-piercing bullet impact, which provides guidance and reference to design protective components and structures.

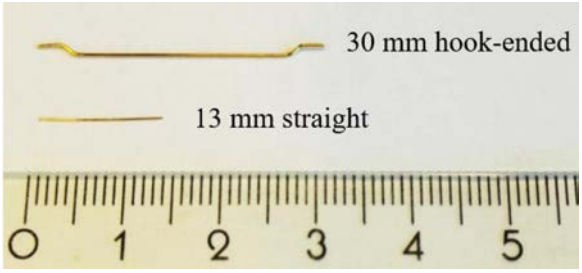

Fig. 1. Utilized steel fibres.

2. Experimental program

2.1. Materials

The ingredients of UHPFRC mixtures included Portland cement (PC), limestone powder (LP), micro-silica (mS), two normal sands with different sizes (S), coarse basalt aggregates (BA) with different sizes, steel fibres with different types (SF), polycarboxylic ethers based superplasticizer (SP) and tap water (W). The detailed physical and chemical properties of powders can be found in our previous studies [25,31]. Two different steel fibres were used, namely 13 mm (short) straight fibre and 30 mm (long) hook-ended fibre, as described in Fig. 1 and Table 1. Fig. 2 shows the particle size distributions (PSD) of powders and aggregates.

2.2. Mix design

Five UHPFRC matrices were designed with the maximum aggregate size (D_{max}) ranging from 2 mm up to 25 mm, as presented in Table 2. 20% limestone powder and 5% micro-silica were added to partially replace the cement by mass, considering both sustainability and performance [25]. The powder content was reduced from 900 kg/m^3 to 700 kg/m^3 with D_{max} increasing from 2 mm to 25 mm, due to the fact that coarse aggregates contribute to less demand of powder in concrete [25,27,32]. The fractions of aggregates were determined based on a modified packing model by applying the Brouwers mix design method [33–35],

$$P(D) = \frac{D^q - D_{min}^q}{D_{max}^q - D_{min}^q} \tag{1}$$

$$RSS = \sum_{i=1}^{n} [P_{mix}(D_i^{i+1}) - P_{target}(D_i^{i+1})]^2 \rightarrow min \tag{2}$$

where D is the particle size. $P(D)$ is the cumulative fraction of all the particles that are smaller than size D. UHPC incorporating coarser aggregates tends to a smaller distribution modulus q [25], and the specific q values and PSD curves of designed UHPFRC matrixes are shown in Fig. 2(b) [25]. The match of the target lines and designed lines confirms the packing quality of the designed mixes. The water and superplasticizer amounts were adjusted to achieve self-compacting.

2.3. Specimens preparation

To investigate the effects of steel fibre type and dosage, matrix strength, coarse aggregate size, slab thickness, and impact velocity on the ballistic resistance, 37 cylindrical specimens were prepared, as listed in Table 3. Partial targets were duplicate to check the experimental variation. The diameter of all targets are fixed at 300 mm, which is much more than 30 times of the projectile diameter, thus achieving a negligible effect of boundary condition [30]. All the samples were cast in mould and covered by plastic film, and demoulded after 24 h. After curing for another 27 days (see details in Table 3), the ballistic tests of all targets were conducted.

Table 1
Characteristics of steel fibres (provided by the manufacturers).

Length, l (mm)	Fibre shape	Diameter, d (mm)	Aspect ratio, l/d	Density (kg/m^3)	Tensile strength (MPa)	Elastic modulus (GPa)	Number of fibres per kg
13	Straight	0.21	62	7850	2750	200	27,000
30	Hook-ended	0.38	79	7850	2300	210	3600

2.4. Testing methods

The tensile splitting and compressive strengths of each target were tested by cubic specimens (100 × 100 × 100 mm^3) following the same curing conditions in Table 3, in accordance with EN 12390-6: 2009 and EN 12390-3: 2009, respectively. The hardboard packing strips in EN 12390-6: 2009 cannot withstand UHPFRC and was thus replaced by steel ones.

The in-service 7.62 × 51 mm NATO armor-piercing bullets were used for the ballistic impact test of UHPFRC targets, as shown in Fig. 3. Two striking velocities of the projectile, recorded by a radar velocity system, were utilized in this study by changing the powder amount in the shell case. The projectile consists of outside brass jacket and inside hard steel core, the steel core penetrates into concrete and brass jacket has a deformable damage (Fig. 3(d)). The 7.62 mm calibre launching device and target supporting frame are presented in Fig. 4. The distance between UHPFRC target and the launching device is around 30 m, based on the NATO standard STANAG 2280 [36]. The target supporting frame is fixed on the ground to avoid any variation or movement. A white paper board is placed behind the supporting frame to witness any probable perforation.

After the ballistic test, the UHPFRC target was cut from the centre of impact point along its longitudinal direction (as semi-cylinder), in order to observe the cross-section damage pattern and measure the penetration depth, as illustrated in Fig. 5. In general, a crater was observed on the impact side, while spalling and scabbing occurred on the rear side. The outside brass jacket was usually destroyed and peeled off during the cratering process, subsequently the hard steel core penetrated deeper alone and created a tunnel. The depth of penetration (DOP) of UHPFRC targets included both crater depth and tunnel depth. The projectile could perforate the thin target directly depending on the quality of concrete and speed of bullet.

3. Results and discussion

3.1. Effect of matrix strength

The DOP is one of the most critical responses of UHPFRC under high-velocity projectile impact, which is inversely related to the compressive strength. To identify the effect of matrix strength, the different matrix strength classes of UHPFRC targets are achieved by different curing regimes without changing other key parameters of the recipes, as illustrated in Table 3. The correlations between DOP and UHPFRC compressive strength are shown in Fig. 6. For a reference UHPFRC mixture (M2 with 2% straight fibres) with normal 27 d water curing after demoulding, the compressive strength reaches to around 143.3 MPa. While, the compressive strength is enhanced to 154.3 MPa with 1-day extra thermal curing (60 °C/80% RH), and further increased up to 162.9 MPa applying the same thermal curing after demoulding but with a duration of 5 days. Additionally, one normal strength concrete target (cement:sand:water = 450:1350:225 by mass) is added to demonstrate the superior bullet resistance of the designed UHPFRC. The normal concrete target has the thickness of 120 mm and diameter of 300 mm, and its compressive strength after 28 days is around 55 MPa. The 843 m/s bullet perforates the normal concrete target and breaks it into several pieces. It demonstrates that the designed UHPFRC has much better bullet impact resistance compared to the normal strength concrete.

For the mixtures with different strength classes, the DOP varies from around 62 mm to 57 mm at the striking velocity of 843 m/s, and between 76 mm and 73 mm under the striking velocity of 926 m/s. Generally, a higher compressive strength tends to a better anti-penetration capacity (smaller DOP), which is in line with other investigations about high-velocity projectile penetration of concretes [37–39]. Furthermore, many representative DOP prediction models, such as the U.S. Army Corps Engineers model, National Defence Research Committee model, and Li and Chen's model, have indicated that DOP is correlated to the square root of compressive strength [19,20,40]. Therefore, the trend lines are regressed and plotted in Fig. 6, as followed by

$$\mathrm{DOP} = k/\sqrt{\sigma_c} + d \tag{3}$$

where k is a content value, d is the diameter of projectile. According to the fitting trend lines, the values of DOP can be further reduced to as low as 55 mm and 69.4 mm at a compressive strength of 180 MPa under the low and high striking velocities, respectively. The improvement degrees of penetration resistance of UHPFRC are very limited,

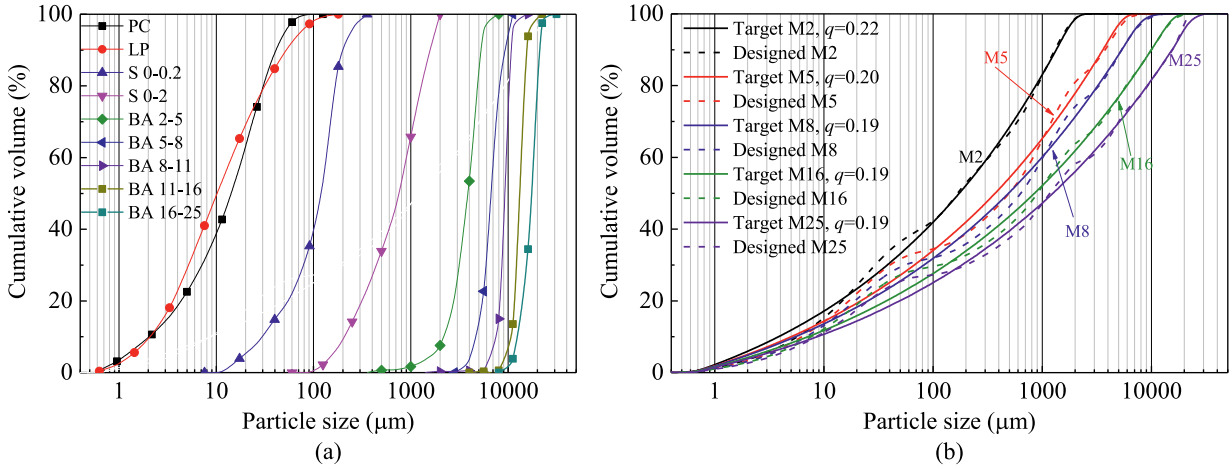

Fig. 2. Particle size distributions of (a) ingredients and (b) designed mixtures.

Table 2
Recipes of designed UHPFRC matrixes (kg/m^3).

Mix.	PC	mS	LP	S0-0.2	S0-2	BA 2-5	BA 5-8	BA 8-11	BA 8-16	BA 16-25	W	SP
M2	675.0	45.0	180	276	1067	–	–	–	–	–	182.0	9.0
M5	637.5	42.5	170	–	988	488	–	–	–	–	174.3	8.5
M8	600.0	40.0	160	–	911	410	249	–	–	–	168.0	8.0
M16	562.5	37.5	150	–	743	390	195	127	192	–	161.3	7.5
M25	525.0	35.0	140	–	667	367	173	121	64	365	154.0	7.0

compared to the UHPFRC mixture with the compressive strength around 150 MPa. It also should be noted that it is relatively easy to develop a ~150 MPa UHPFRC, while a too high strength (e.g. 200 MPa) usually considerably sacrifices the cost and needs extra special treatments, such as very low water amount with a very high dosage of superplasticizer, a large amount cement, a high steel fibre addition, thermal and chemical activation, and extra pressurization treatment before final setting. Hence, it is not efficient to use too high-strength UHPFRC mixtures to develop protective elements by comprehensively considering both cost and anti-penetration performance. Based on the analysis above, we suggest the desired compressive strength of around 150 MPa for the bullet impact resistant UHPFRC.

3.2. Effect of steel fibre type and content

3.1.1. Mechanical strengths

The mechanical strengths of UHPFRC are influenced by the steel fibre types and contents, thus affecting the impact resistance [41–43]. Fig. 7 shows the compressive and splitting tensile strength of UHPFRC mixture (matrix M2, Table 3) with different types and contents of steel fibres. Normally, hook-ended steel fibres with appropriate length are more suitable to reinforce the mechanical properties especially for flexural strength, compared to shorter straight ones [44,45]. UHPFRC incorporating short straight fibres possesses slightly higher compressive and splitting tensile strengths. This is probably attributed to the more homogenous distribution of the smaller fibres in matrix, thus providing a better reinforcement. The compressive strength continuously increases from 130.9 MPa to 177.2 MPa when adding the straight fibre content from 0 to 5%, while the splitting tensile strength ranges between 9.5 MPa and 25.7 MPa. Namely, the improvement ratios in the presence of 5% straight fibres are 35.4% and 170.5% for compressive and splitting tensile strengths, respectively. The different reinforcing effects on compressive and tensile strengths probably indicate that the steel fibre addition preferably improves the crack inhibition capacity rather than anti-penetration, which will be discussed in the following sections. The phenomenon is in line with Kravanja et al. [46,47], even they used the different types of projectile with a lower striking velocity.

3.1.2. Depth of penetration

The steel fibres in UHPFRC enhance the bullet impact resistance by inhibiting crack propagation, diminishing the secondary harm induced by the scabbing and spalling fragments, and providing confinement to the inner local impact position. Fig. 8 presents the DOP of the designed UHPFRC targets with two kinds of high-strength steel fibres at a bullet impact velocity of 843 m/s. The DOP of the plain target without fibre is very large, namely 78 mm. While, it sharply decreases to 66 mm and 62 mm when adding 1% 30 mm hook-ended and 13 mm straight steel fibres, namely 15.4% and 20.5% reductions, respectively. After that, the penetration resistance can be further gradually improved with the increase of steel fibres' dosage, e.g. a DOP of 61 mm is achieved with 3% hook-ended fibres and 58 mm with 5% straight ones. But, steel fibre addition beyond 1% seems to have a limited contribution to decrease the DOP, especially in the case of the 13 mm straight fibres. Further, some other researchers also indicated that too high content of fibres does not contribute too much penetration resistance [48].

It should be pointed out that the utilization of 13 mm straight fibres seems to be more efficient to reinforce the bullet penetration resistance than the 30 mm hook-ended ones, although a long and hook shape in some cases results in better mechanical properties (e.g. flexural strength) in UHPFRC [44,45]. Yu et al. also revealed a similar high-velocity projectile experimental result, where the DOP is smaller with hybrid fibres (0.5% small and 1.5% large) compared to the pure 2% large ones [49]. On the one hand, the smaller DOP for UHPFRC target with straight fibres is attributed to the higher compressive and tensile strengths, as illustrated in Fig. 7. On the other hand, the number density (number of fibres per kg) of straight fibre is much larger and the fibres can be distributed more homogeneously. It means that the projectile has more possibility to strike the high-strength fibres, and consequently being subjected to heavier mass abrasion and penetration resistance. Thus, the 13 mm straight fibres are recommended for bullet resistant UHPFRC.

3.1.3. Damage patterns

As analysed above, 1% of 13 mm straight steel fibres are able to contribute enough penetration resistance of the designed UHPFRC targets. Nevertheless, a protective UHPFRC element also needs to possess good crack resistance, in order to remain sufficient residual bearing capacity and relieve second harm induced by the scabbing and spalling fragments. Therefore, the damage patterns of UHPFRC are observed with a different straight steel fibre content, through spraying the damage surfaces with white paint to make cracks more visible, as illustrated in Fig. 9.

Table 3
UHPFRC targets for four groups.

Groups	Matrix No.	Thickness (mm)	Impact velocity (m/s)	Fiber type & dosage (vol.)	Curing regime
Matrix strength effect	M2	120	843, 926	2% straight	1 d heat curing (60 °C/80 RH), 26 d water curing. 5 d heat curing (60 °C/80 RH), 22 d water curing.
Fibre effect	M2	120	843	0 1%, 2%, 3%, 5% straight 1%, 2%, 3% hook-ended	27 d water curing
Aggregate size effect	M5 M8 M16 M25	100	843, 926	2% straight	27 d water curing
Thickness effect	M2	60 ~ 140	843, 926	2% straight	27 d water curing

Note: 1% of steel fibres by volume of matrix is around 78.5 kg/m^3.

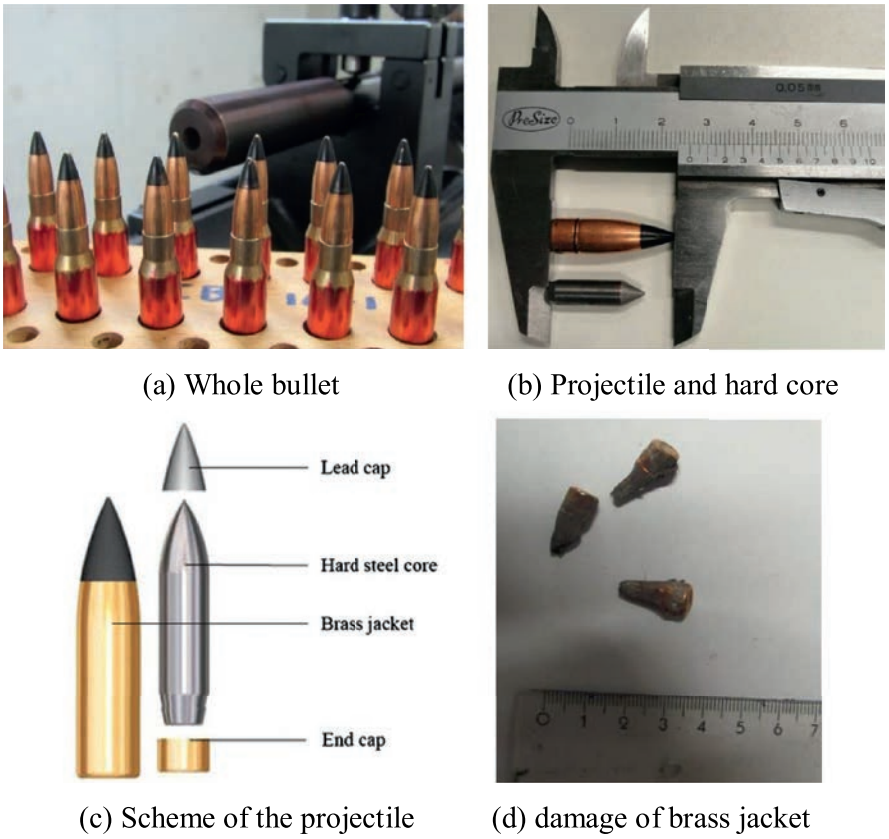

Fig. 3. 7.62 × 51 mm NATO armor-piercing bullet.

The plain target is extremely brittle and split into several pieces, which indicates that it cannot withstand the bullet impact. 1% steel fibres result in an integral specimen and no obvious scabbing on the rear side due to its bridging effect and energy absorption capacity [50], but a relatively large crater and many macro cracks are observed on the impact side, as shown in Fig. 9(b). 2% steel fibres considerably diminish the crater diameter and only some hairline cracks are visible. A higher content of steel fibres usually contributes to a higher tensile strength, larger strain hardening capacity and energy absorption, which thus lead to a better crack resistance [51]. As illustrated in Fig. 9, continuously increasing the utilized fibre content can further improve the crack inhibition capacity, e.g. almost no visible crack is seen with fibres up to 5%, however the crater diameter remains similar.

To sum up, the steel fibres are indispensable and play a critical role in UHPFRC towards both penetration and crack resistance when subjected to high-velocity bullet impact. 2% of 13 mm straight steel fibres are suggested by comprehensively considering DOP, damage pattern and fibre utilization efficiency, which is in line with the suggestion on fibre content for thin UHPFRC targets under deformable projectile impact [52].

3.3. Effect of coarse aggregate

3.3.1. Mechanical strengths

Fig. 10 shows the mechanical strengths of UHPFRC incorporating different D_{max} in the presence of 2% of 13 mm straight steel fibres. For the UHPFRC with D_{max} of 2 mm (sands), the 28 d compressive and splitting tensile strengths attain 143.3 MPa and 15.8 MPa, respectively. The strengths fluctuate between 155.5–165.6 MPa and 17.5–19.1 MPa, respectively, when coarse basalt aggregates are introduced with D_{max} from 5 mm to 25 mm. The coarser aggregates utilization in UHPFRC usually tends to a slightly lower mechanical strength [25,28]. The

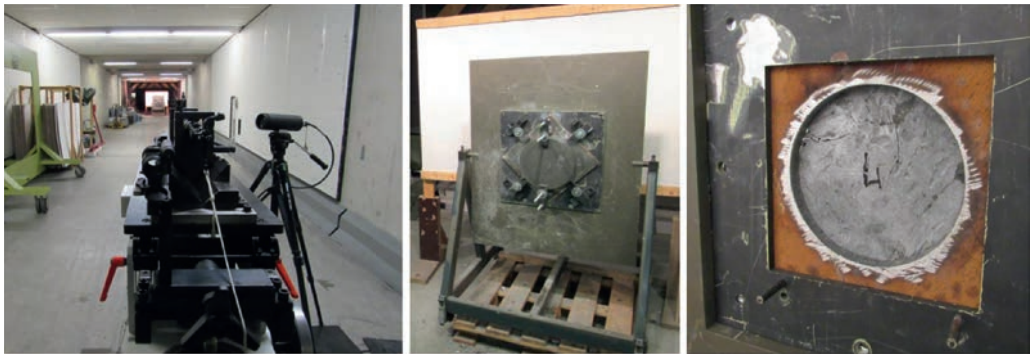

Fig. 4. Launching device (a), and front (b) and rear (c) side of target.

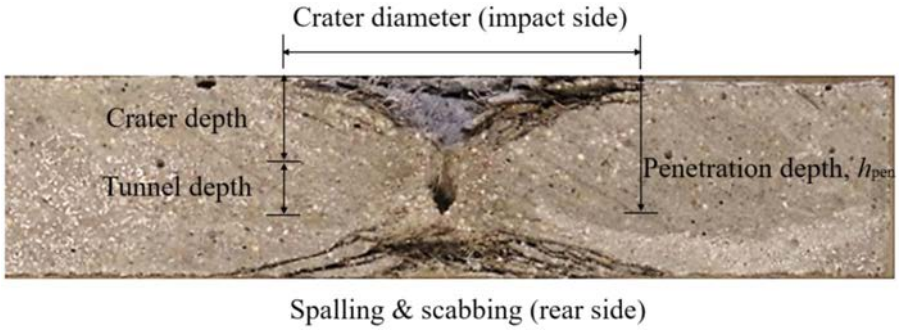

Fig. 5. Typical damage pattern of UHPFRC target.

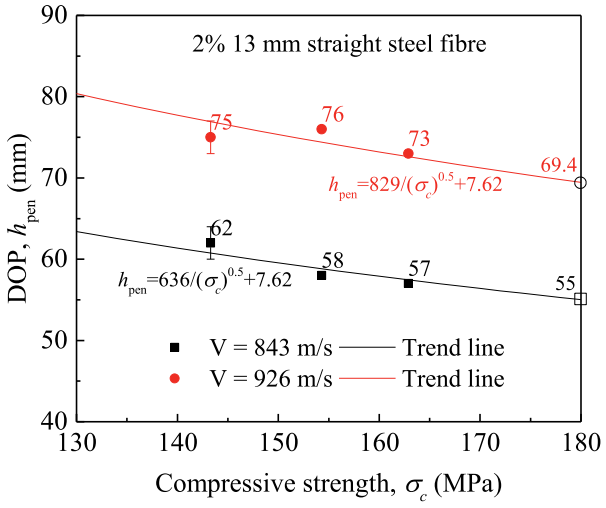

Fig. 6. Correlation between DOP and matrix strength.

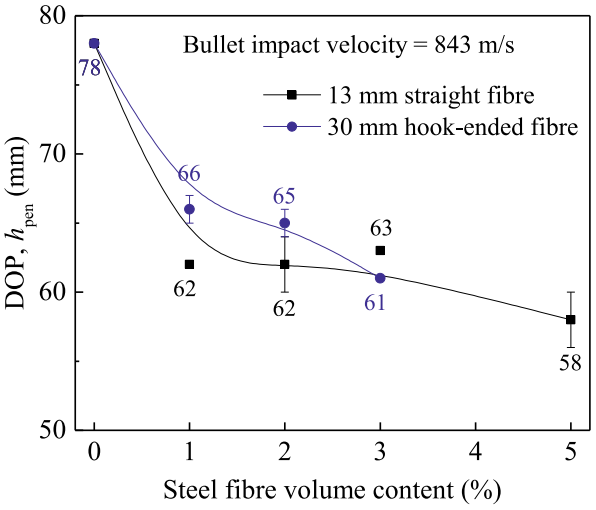

Fig. 8. DOP of UHPFRC targets with different steel fibres.

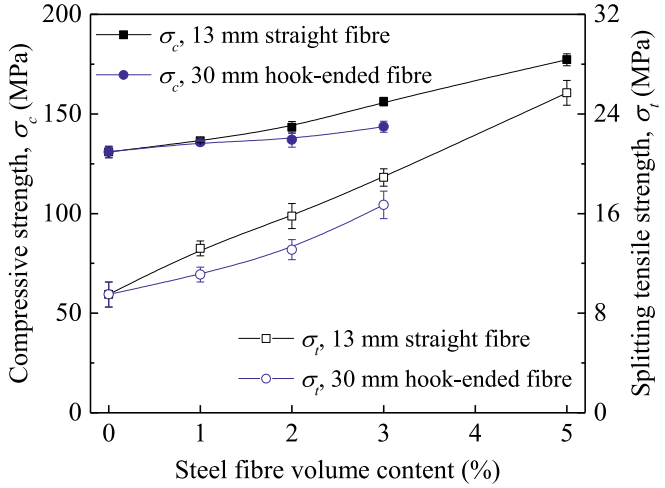

Fig. 7. Mechanical strengths of UHPFRC with different steel fibres.

enhanced mechanical properties are probably mainly owed to the lower absolute water amount, as presented in Table 2, which tends to reduce the porosity and consequently increases the packing density.

Based on the packing of used particle size distribution, Eqs (1) and (2), a lower fines content is needed for a mixture with coarser particles. In this study, the powder content decreases from 900 kg/m^3 to 700 kg/m^3 with the increase of D_{max} from 2 mm to 25 mm. Although the active binders are diluted, the mechanical strength of UHPFRC is not sacrificed. Apart from the increased packing density as mentioned above, the higher water-to-binder ratio for UHPFRC incorporating coarser aggregates contributes to improving the binder hydration degree, and thus compensating the reduction effect of absolute powder amount. Hence, introducing high-strength coarse aggregates improves the cement utilization and economic benefit, without sacrificing or even strengthening mechanical strength.

3.3.2. Depth of penetration

Many researchers believed that high-strength coarse aggregates are beneficial for diminishing the DOP under high-velocity projectile impact, due to mass abrasion, trajectory deviation of the projectile [20,29,30,37,53]. Furthermore, in the presence of hard coarse aggregates in UHPFRC under impact loading, more fracture energy is dissipated because more cracks go through the aggregates instead of initiating along the interfacial transition zones [5,54]. But some researchers pointed out that this finding is questionable when the projectile is very small (e.g. 7.62 mm [55,56]) relative to the size of aggregates [57], because of the high variability of striking on whether aggregate or mortar [19]. Fig. 11 shows the DOP of UHPFRC targets with different D_{max} by the in-service 7.62 × 51 mm NATO armor-piercing bullets. When increasing D_{max} from 2 mm to 25 mm, the values of DOP reduce from about 62 mm to 53 mm and from 75 mm to 64.5 mm under 843 m/s and 926 m/s impact, respectively. Namely, the reduction ratios are approximately 14.5%, which is more efficient and cost-effective compared to the measure of fibre addition, as illustrated in Fig. 8. The enhanced anti-penetration capacity of UHPFRC is attributed to both the enlarged D_{max} and the concomitantly increased volume content of hard basalt aggregates. Wu et al. [29] suggested the hard coarse aggregate size should be larger than 1.5 times of the projectile diameter. Wang et al. [19] demonstrated critical contribution of the coarse aggregate volume fraction (φ) and the hardness (η). Both the

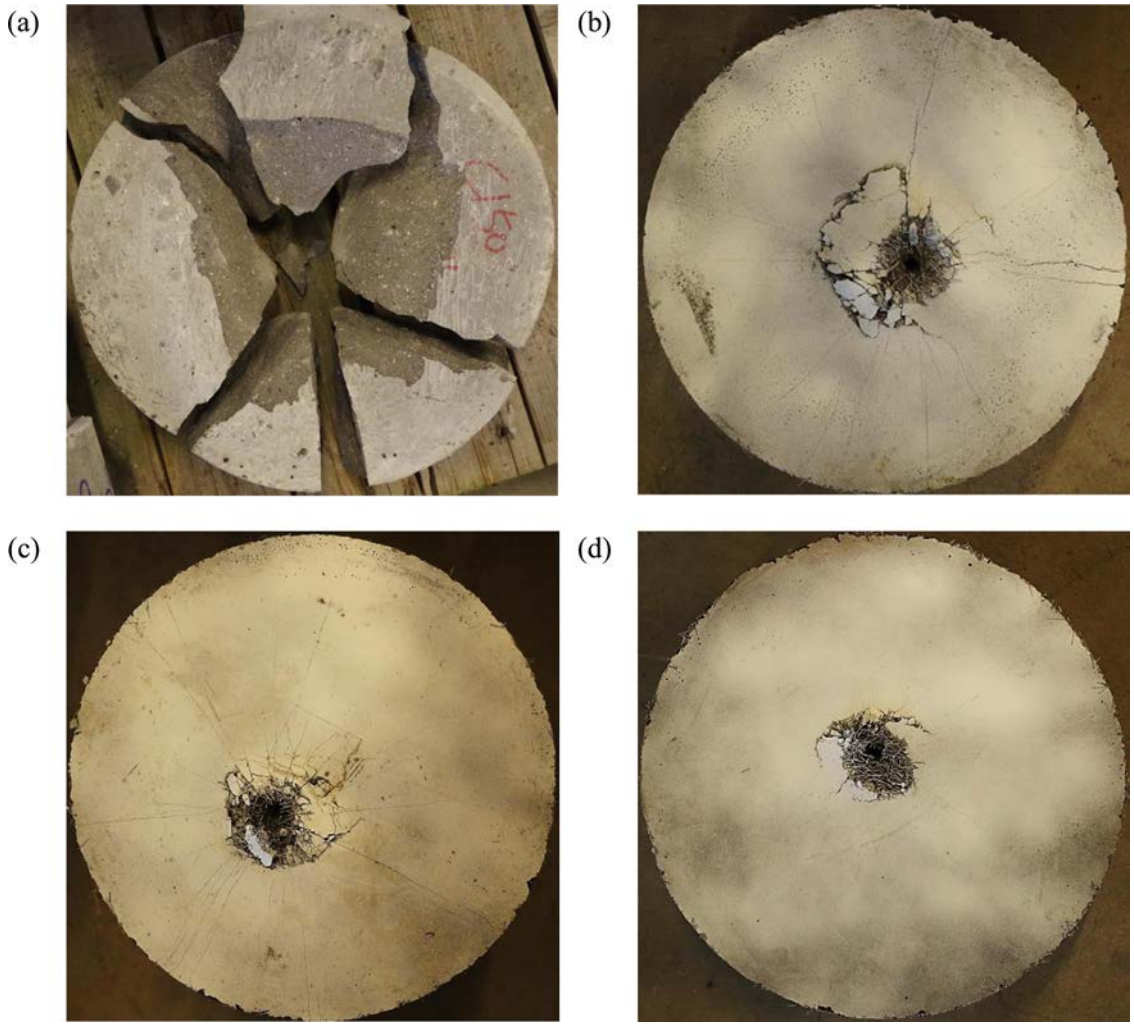

Fig. 9. Damage patterns with different straight fibre contents: (a) 0, (b) 1%, (c) 2%, (d) 5% (diameter = 300 mm).

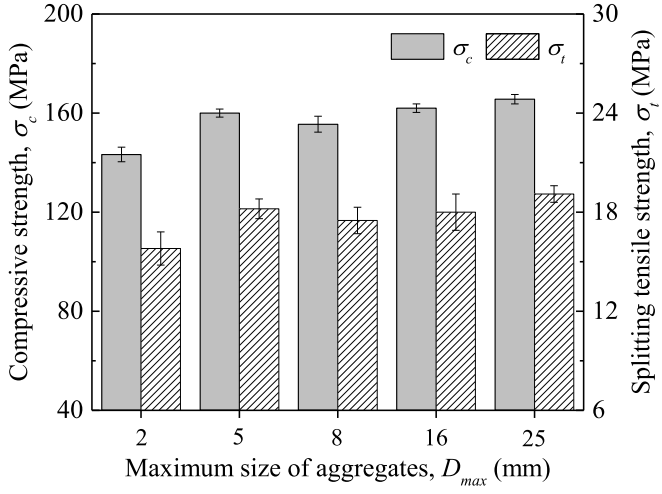

Fig. 10. Mechanical strengths of UHPFRC with different D_{max}.

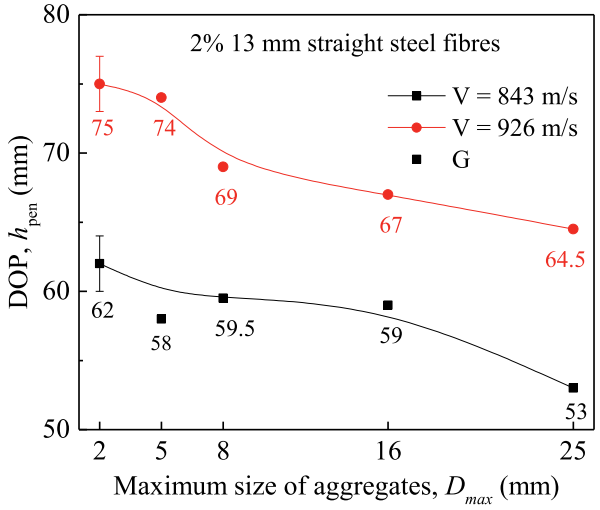

Fig. 11. DOP of UHPFRC targets with different D_{max}.

volume fraction (φ) and the hardness (η) contribute to the total effective hardness index, and this index has inversely linear relationship with the DOP. The basalt aggregates usually have much higher hardness than cementitious based mortar, which means that introducing coarse basalt aggregates contributes to the total effective hardness index and then reduces DOP. Thus, UHPFRC incorporating D_{max} of 25 mm is suggested to develop protective elements by considering positive effects of both size and volume fraction of basalt aggregates.

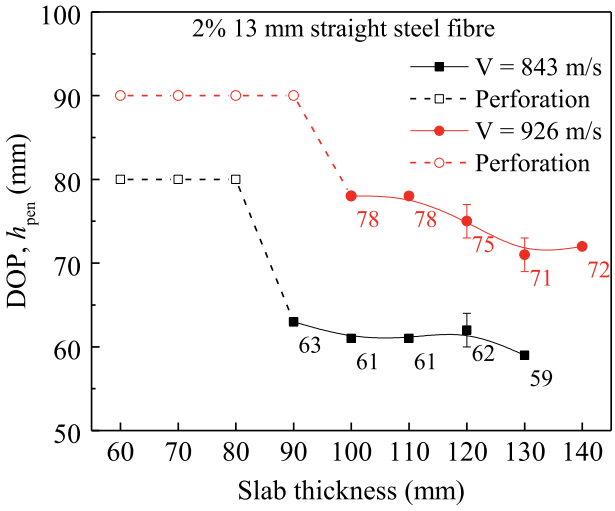

Fig. 12. DOP and perforation limit of concrete (M2) with different target thicknesses.

3.4. Effect of target thickness

3.4.1. Perforation limit

The perforation limit is defined as the minimum safe thickness of a target to avoid the perforation under a specific projectile impact with a given striking velocity [39,58]. The perforation limit has great significance for developing protective structures, which could provide guidance for engineers to design the safe and cost-efficient structures [59–61]. In this paper, the perforation limit of the designed UHPFRC is determined from the damage observations of the targets with different thicknesses. Fig. 12 presents the DOP of UHPFRC targets (M2) with different thicknesses from 60 mm to 140 mm under striking velocities of 843 m/s and 926 m/s. For a lower striking velocity of 843 m/s, the DOP is slightly enlarged from about 59 mm to 63 mm with the decrease of the target thickness from 130 mm to 90 mm. After that, the UHPFRC target is perforated in the case of the thickness down to 80 mm, as represented by the dash line. For a higher striking velocity of 926 m/s, the DOP experiences a similar decreasing tendency, and the perforation phenomenon occurs at the thickness of 90 mm. The accurate perforation limit cannot be directly measured due to the testing thickness interval of being 10 mm. Thus, the perforation limit is calculated as the average thicknesses of the thickest perforated target and the thinnest unperforated target. In this study, the perforation limits of the designed

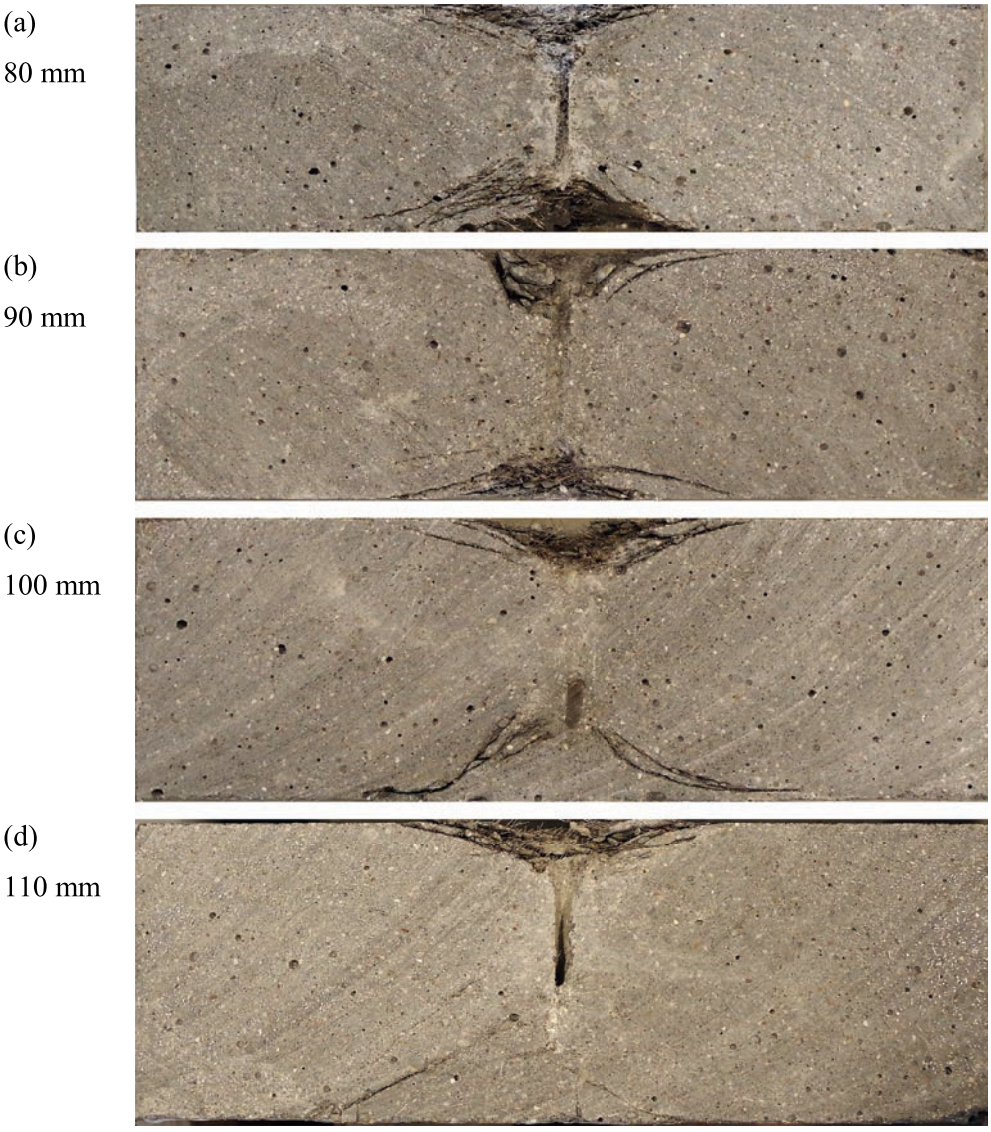

Fig. 13. Cross-sections damage of concrete (M2) with different target thicknesses at 926 m/s, diameter = 300 mm.

UHPFRC subjected to the in-service 7.62 × 51 mm NATO armor-piercing bullet are derived as 85 mm and 95 mm for a given striking velocity of 843 m/s and 926 m/s, respectively.

3.4.2. Damage patterns

To reveal the mechanism of target thickness effect on high-velocity bullet impact resistance, the cross-section damage patterns of UHPFRC targets with different thicknesses are observed by cutting the tested samples into semi-cylinders. Because the effects of target thickness on damage patterns at 843 m/s and 926 m/s share the same tendency, we only present those at the higher striking velocity in this paper, as illustrated in Fig. 13.

The targets with the thickness of both 80 mm and 90 mm are all perforated. While, the damage of the thinner target is much severer, namely larger crater diameter and larger depth on the impact side, and more spalling and scabbing on the rear side. When the target thickness increases up to 100 mm, the inner hard core of projectile is stopped inside the target. There is no obvious spalling and scabbing on the rear side, but two dominant macro cracks like inverted funnel are still observed inside the target. The crack resistance can be further improved with the increase of the thickness, for example a much smaller crater and no obvious macro cracks are observed in the case of 110 mm target. The diminished damage degree of a thicker UHPFRC target is attributed to a more remarkable confinement of outer concrete on the inner local damage part. The impact bearing capacity of concrete can be enhanced with confinement [62–64], which consequently reduces the concrete damage degree, as well as the DOP shown in Fig. 12.

4. Conclusions

This paper investigates the key parameters of UHPFRC towards the high-velocity impact resistance by in-service 7.62 × 51 mm NATO armor-piercing bullets. The main key parameters on penetration and crack resistance are studied, including matrix strength, steel fibre type and content, aggregate size and target thickness. The present findings contribute to providing reference and guidance to design the protective elements and structures. Based on the obtained results, the following conclusions can be summarized:

- The designed UHPFRC with the compressive strength of 140 − 170 MPa by using a particle packing model shows excellent high-velocity bullet impact resistance, and the compressive strength class of 150 MPa is recommended for UHPFRC to design protective structures by considering both cost efficiency and anti-penetration performance.
- Steel fibres are indispensable and play a critical role in UHPFRC towards bullet impact resistance, and 13 mm straight steel fibres show better contributions than 30 mm hook-ended ones. 2% is recommended as the optimum content to design impact resistant UHPFRC by further concerning the crack inhibition.
- Coarse basalt aggregates with particle size up to 25 mm are successfully introduced into protective UHPFRC system, which results in a lower powder consumption (i.e. from 900 kg/m^3 to 700 kg/m^3) and lower cost, higher mechanical strength and stronger bullet impact resistance. The DOP reduction is about 14.5% with the increase of the D_{max} from 2 mm to 25 mm.
- A UHPFRC target with a larger thickness tends to a smaller DOP, attributed to the better confinement of outer material to the local damaged concrete. Perforation limits (safe thicknesses) of the designed UHPFRC (M2, Table 3) are about 85 mm and 95 mm to withstand the 7.62 × 51 mm NATO armor-piercing bullet at the striking velocity of 843 m/s and 926 m/s, respectively.

Declaration of Competing Interest

The authors declare that they have no known competing financial interests or personal relationships that could have appeared to influence the work reported in this paper.

Acknowledgements

This research was conducted under the funding of the China Scholarship Council and Eindhoven University of Technology. The authors thank late Ing. Ad. Verhagen for discussion on impact resistant concrete. We are grateful for the help of Ing. D. Krabbenborg for the ballistic tests. Appreciations are expressed to the Dutch Defense Academy and Knowledge Centre Weapon System, and Ammunition from the Dutch Ministry of Defense for conducting the ballistic tests. The ENCI, Bekaert and Sika are acknowledged for supplying the cement, steel fibres and superplasticizer, respectively.

References

[1] Soufeiani L, Raman SN, Bin JMZ, Alengaram UJ, Ghadyani G, Mendis P. Influences of the volume fraction and shape of steel fibers on fiber-reinforced concrete subjected to dynamic loading – a review. Eng Struct 2016;124:405–17.
[2] Tran NT, Tran TK, Jeon JK, Park JK, Kim DJ. Fracture energy of ultra-high-performance fiber-reinforced concrete at high strain rates. Cem Concr Res 2015;79:169–84.
[3] Wang D, Shi C, Wu Z, Xiao J, Huang Z, Fang Z. A review on ultra high performance concrete: part II. Hydration, microstructure and properties. Constr Build Mater 2015;96:368–77.
[4] Yu R, Spiesz P, Brouwers HJH. Static properties and impact resistance of a green Ultra-High Performance Hybrid Fibre Reinforced Concrete (UHPHFRC): experiments and modeling. Constr Build Mater 2014;68:158–71.
[5] Li PP, Yu QL. Responses and post-impact properties of ultra-high performance fibre reinforced concrete under pendulum impact. Compos Struct 2019;208:806–15.
[6] Kang S-T, Lee Y, Park Y-D, Kim J-K. Tensile fracture properties of an Ultra High Performance Fiber Reinforced Concrete (UHPFRC) with steel fiber. Compos Struct 2010;92:61–71.
[7] Liu J, Wu C, Su Y, Li J, Shao R, Chen G, et al. Experimental and numerical studies of ultra-high performance concrete targets against high-velocity projectile impacts. Eng Struct 2018;173:166–79.
[8] Feng J, Sun W, Liu Z, Cui C, Wang X. An armour-piercing projectile penetration in a double-layered target of ultra-high-performance fiber reinforced concrete and armour steel: experimental and numerical analyses. Mater Des 2016;102:131–41.
[9] Richard P, Cheyrezy M. Composition of reactive powder concretes. Cem Concr Res 1995;25:1501–11.
[10] de Larrard F, Sedran T. Optimization of ultra-high-performance concrete by the use of a packing model. Cem Concr Res 1994;24:997–1009.
[11] Wille K, Naman AE, Parra-Montesinos GJ. Ultra-High performance concrete with compressive strength exceeding 150MPa (22ksi): a simpler way. ACI Mater J 2011;108:46–53.
[12] Shi C, Wu Z, Xiao J, Wang D, Huang Z, Fang Z. A review on ultra high performance concrete: part I. raw materials and mixture design. Constr Build Mater 2015;96:368–77.
[13] Yoo DY, Banthia N. Mechanical properties of ultra-high-performance fiber-reinforced concrete: a review. Cem Concr Compos 2016;73:267–80.
[14] Feng J, Li W, Wang X, Song M, Ren H, Li W. Dynamic spherical cavity expansion analysis of rate-dependent concrete material with scale effect. Int J Impact Eng 2015;84:24–37.
[15] Su H, Xu J. Dynamic compressive behavior of ceramic fiber reinforced concrete under impact load. Constr Build Mater 2013;45:306–13.
[16] Zhang X, Ruiz G, Abd Elazim AM. Loading rate effect on crack velocities in steel fiber-reinforced concrete. Int J Impact Eng 2015;76:60–6.
[17] Ren F, Mattus CH, Wang JJA, DiPaolo BP. Effect of projectile impact and penetration on the phase composition and microstructure of high performance concretes. Cem Concr Compos 2013;41:1–8.
[18] Lai J, Guo X, Zhu Y. Repeated penetration and different depth explosion of ultra-high performance concrete. Int J Impact Eng 2015;84:1–12.
[19] Wang S, Le HTN, Poh LH, Feng H, Zhang MH. Resistance of high-performance fiber-reinforced cement composites against high-velocity projectile impact. Int J Impact Eng 2016;95:89–104.
[20] Zhang MH, Shim VPW, Lu G, Chew CW. Resistance of high-strength concrete to projectile impact. Int J Impact Eng 2005;31:825–41.
[21] Li PP, Cao YYY, Brouwers HJH, Chen W, Yu QL. Development and properties evaluation of sustainable ultra-high performance pastes with quaternary blends. J Clean Prod 2019;240:118124.
[22] Cao YYY, Li PP, Brouwers HJH, Sluijsmans M, Yu QL. Enhancing flexural performance of ultra-high performance concrete by an optimized layered-structure concept. Compos Part B Eng 2019;171:154–65.
[23] Yoo D-Y, Lee J-H, Yoon Y-S. Effect of fiber content on mechanical and fracture properties of ultra high performance fiber reinforced cementitious composites. Compos Struct 2013;106:742–53.
[24] Wu Z, Shi C, He W, Wu L. Effects of steel fiber content and shape on mechanical properties of ultra high performance concrete. Constr Build Mater 2016;103:8–14.

[25] Li PP, Yu QL, Brouwers HJH. Effect of coarse basalt aggregates on the properties of Ultra-High Performance Concrete (UHPC). Constr Build Mater 2018;170:649–59.
[26] Liu J, Han F, Cui G, Zhang Q, Lv J, Zhang L, et al. Combined effect of coarse aggregate and fiber on tensile behavior of ultra-high performance concrete. Constr Build Mater 2016;121:310–8.
[27] Dittmer T, Beushausen H. The effect of coarse aggregate content and size on the age at cracking of bonded concrete overlays subjected to restrained deformation. Constr Build Mater 2014;69:73–82.
[28] Li PP, Yu QL, Brouwers HJH, Chen W. Conceptual design and performance evaluation of two-stage ultra-low binder ultra-high performance concrete. Cem Concr Res 2019;125:105858.
[29] Wu H, Fang Q, Gong J, Liu JZ, Zhang JH, Gong ZM. Projectile impact resistance of corundum aggregated UHP-SFRC. Int J Impact Eng 2015;84:38–53.
[30] Wu H, Fang Q, Chen XW, Gong ZM, Liu JZ. Projectile penetration of ultra-high performance cement based composites at 510–1320m/s. Constr Build Mater 2015;74:188–200.
[31] Li PP, Yu QL, Brouwers HJH. Effect of PCE-type superplasticizer on early-age behaviour of ultra-high performance concrete (UHPC). Constr Build Mater 2017;153:740–50.
[32] Banyhussan QS, Yıldırım G, Bayraktar E, Demirhan S, Şahmaran M. Deflection-hardening hybrid fiber reinforced concrete: the effect of aggregate content. Constr Build Mater 2016;125:41–52.
[33] Brouwers HJH, Radix HJ. Self-compacting concrete: theoretical and experimental study. Cem Concr Res 2005;35:2116–36.
[34] Brouwers HJH. Particle-size distribution and packing fraction of geometric random packings. Phys Rev E 2006;74:031309.
[35] Yu QL, Spiesz P, Brouwers HJH. Development of cement-based lightweight composites - Part 1: mix design methodology and hardened properties. Cem Concr Compos 2013;44:17–29.
[36] STANAG 2280. Test procedures and classification of the effects of weapons on structures. North Atlantic Treaty Organization (NATO); 2009.
[37] Lai J, Wang H, Yang H, Zheng X, Wang Q. Dynamic properties and SPH simulation of functionally graded cementitious composite subjected to repeated penetration. Constr Build Mater 2017;146:54–65.
[38] Mao L, Barnett S, Begg D, Schleyer G, Wight G. Numerical simulation of ultra high performance fibre reinforced concrete panel subjected to blast loading. Int J Impact Eng 2014;64:91–100.
[39] Hanchak SJ, Forrestal MJ, Young ER, Ehrgott JQ. Perforation of concrete slabs with 48MPa (7 ksi) and 140MPa (20 ksi) unconfined compressive strengths. Int J Impact Eng 1992;12:1–7.
[40] Li QM, Chen XW. Dimensionless formulae for penetration depth of concrete target impacted by a non-deformable projectile. Int J Impact Eng 2003;28:93–116.
[41] Ong KCG, Basheerkhan M, Paramasivam P. Behaviour of fibre reinforced concrete slabs under low velocity projectile impact. ACI Spec Publ 1999;172:993–1011.
[42] Feng J, Gao X, Li J, Dong H, He Q, Liang J, et al. Penetration resistance of hybrid-fiber-reinforced high-strength concrete under projectile multi-impact. Constr Build Mater 2019;202:341–52.
[43] Feng J, Gao X, Li J, Dong H, Yao W, Wang X, et al. Influence of fiber mixture on impact response of ultra-high-performance hybrid fiber reinforced cementitious composite. Compos Part B Eng 2019;163:487–96.
[44] Yoo DY, Kang ST, Yoon YS. Enhancing the flexural performance of ultra-high-performance concrete using long steel fibers. Compos Struct 2016;147:220–30.
[45] Yu R, Spiesz P, Brouwers HJH. Development of Ultra-High Performance Fibre Reinforced Concrete (UHPFRC): towards an efficient utilization of binders and fibres. Constr Build Mater 2015;79:273–82.
[46] Kravanja S, Sovják R. Ultra-high-performance fibre-reinforced concrete under high-velocity projectile impact. Part I. experiments. Acta Polytech 2018;58:232–9.
[47] Kravanja S, Sovják R, Konrád P, Zatloukal J. Penetration resistance of semi-infinite UHPFRC targets with various fiber volume fractions against projectile impact. Procedia Eng 2017;193:112–9.
[48] Máca P, Sovják R, Konvalinka P. Mix design of UHPFRC and its response to projectile impact. Int J Impact Eng 2014;63:158–63.
[49] Yu R, Spiesz P, Brouwers HJH. Energy absorption capacity of a sustainable Ultra-High Performance Fibre Reinforced Concrete (UHPFRC) in quasi-static mode and under high velocity projectile impact. Cem Concr Compos 2016;68:109–22.
[50] Caverzan A, Cadoni E, Di Prisco M. Tensile behaviour of high performance fibre-reinforced cementitious composites at high strain rates. Int J Impact Eng 2012;45:28–38.
[51] Park SH, Kim DJ, Ryu GS, Koh KT. Tensile behavior of ultra high performance hybrid fiber reinforced concrete. Cem Concr Compos 2012;34:172–84.
[52] Sovják R, Shanbhag D, Konrád P, Zatloukal J. Response of thin UHPFRC targets with various fibre volume fractions to deformable projectile impact. Procedia Eng 2017;193:3–10.
[53] Liu J, Wu C, Li J, Fang J, Su Y, Shao R. Ceramic balls protected ultra-high performance concrete structure against projectile impact–A numerical study. Int J Impact Eng 2019;125:143–62.
[54] Tai YS, El-Tawil S, Chung TH. Performance of deformed steel fibers embedded in ultra-high performance concrete subjected to various pullout rates. Cem Concr Res 2016;89:1–13.
[55] Peng Y, Wu H, Fang Q, Liu JZ, Gong ZM. Impact resistance of basalt aggregated UHP-SFRC/fabric composite panel against small caliber arm. Int J Impact Eng 2016;88:201–13.
[56] Sovják R, Vavřiník T, Zatloukal J, Máca P, Mičunek T, Frydrýn M. Resistance of slim UHPFRC targets to projectile impact using in-service bullets. Int J Impact Eng 2015;76:166–77.
[57] Peng Y, Wu H, Fang Q, Gong ZM. Geometrical scaling effect for penetration depth of hard projectiles into concrete targets. Int J Impact Eng 2018;120:46–59.
[58] Dancygier AN, Katz A, Benamou D, Yankelevsky DZ. Resistance of double-layer reinforced HPC barriers to projectile impact. Int J Impact Eng 2014;67:39–51.
[59] Peng Y, Wu H, Fang Q, Liu JZ, Gong ZM. Residual velocities of projectiles after normally perforating the thin ultra-high performance steel fiber reinforced concrete slabs. Int J Impact Eng 2016;97:1–9.
[60] Li J, Zhang YX. Evolution and calibration of a numerical model for modelling of hybrid-fibre ECC panels under high-velocity impact. Compos Struct 2011;93:2714–22.
[61] Tai YS. Flat ended projectile penetrating ultra-high strength concrete plate target. Theor Appl Fract Mech 2009;51:117–28.
[62] Chi Y, Xu L, Mei G, Hu N, Su J. A unified failure envelope for hybrid fibre reinforced concrete subjected to true triaxial compression. Compos Struct 2014;109:31–40.
[63] Song D, Tan Q, Zhan H, Liu F, Jiang Z. Experimental investigation on the cellular steel-tube-confined concrete targets against projectile impact. Int J Impact Eng 2019;131:94–110.
[64] Meng C, Tan Q, Jiang Z, Song D, Liu F. Approximate solutions of finite dynamic spherical cavity-expansion models for penetration into elastically confined concrete targets. Int J Impact Eng 2018;114:182–93.